Cell Adhesion Phenotype Library with Photonic Crystal Enhanced Microscopy

Yue Zhuo[1,4], Ji Sun Choi[2,5], Thibault Marin[6], Hojeong Yu[3], Brendan A. Harley[2,5], Brian T. Cunningham[1,3,4,5*]
[1]Department of Bioengineering, [2]Department of Chemical and Biomolecular Engineering; [3]Department of Electrical and Computer Engineering, [4]Micro and Nanotechnology Laboratory, [5]Carl R. Woese Institute for Genomic Biology, [6]Research Park, University of Illinois at Urbana-Champaign, Urbana, Illinois 61801, USA
E-mail address: bcunning@illinois.edu

Abstract: We apply PCEM to investigate adhesion of different types of stem cells and cancer cells as a cell adhesion phenotype library. The imaging and analysis results presented here provide a new tool for biologists to gain a deeper understanding of the fundamental mechanisms involved with cell adhesion and concurrent migration events.
OCIS codes: (280.1415) Biological sensing and sensors; (050.5298) Photonic crystals; (170.0180) Microscopy

1. Introduction

Cell adhesion, the means by which cells communicate with neighboring cells and the surrounding matrix *in vivo*, is critical for maintaining normal cell functions during homeostasis. Cell adhesion not only provides structural support, but also contributes to functional processes crucial for proliferation and survival. It is highly desirable to collect cell adhesion-related information of single cells to delineate the role of adhesion and elucidate the associated biological mechanisms. We employ Photonic Crystal Enhanced Microscopy (PCEM), a label-free microscopy approach with near-field imaging on nano structured dielectric surfaces and associated advanced data analysis, to study cell-surface interactions [1-5]. PCEM offers a platform for quantitative and dynamic imaging of cell adhesion by measuring changes occurring only at the cell-surface interface (<200 nm in thickness) arising from cellular effective mass density redistribution associated changes with adhesion events. PCEM utilizes the cell membrane and its associated protein components as an integral part of the photonic crystal (PC) structure. The PC surface is a subwavelength nano structured material with a periodic modulation of refractive index that acts as a narrow bandwidth resonant optical reflector at one specific wavelength and incident angle. The high reflection efficiency of the PC at the resonant wavelength/angle combination is the result of the formation of electromagnetic standing waves on its surface that extend into the surrounding medium in the form of an evanescent electromagnetic field.

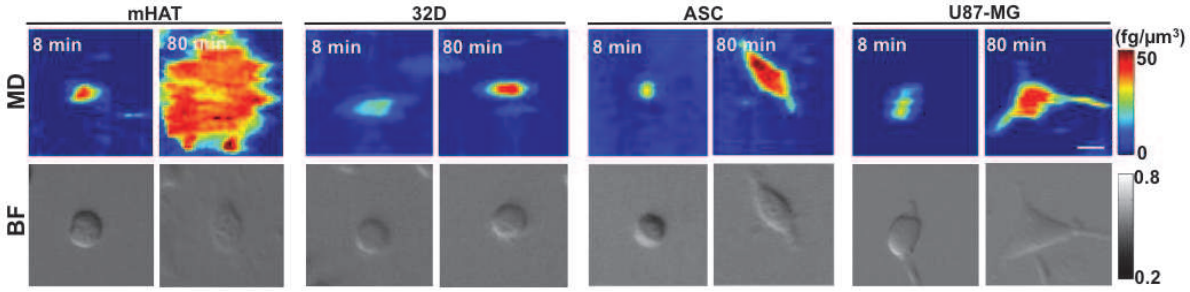

Fig. 1. Membrane-associated effective mass density (MD) images of three different types of stem cells and one type of cancer cells: mHAT (dental stem cell), 32D (myeloid stem cell), ASC (adipose stem cell), U87-MG (brain cancer cell). Bar length = 10 μm.

2. Methods

The PCEM instrument is a modified brightfield microscope that uses a line-scanning approach to measure the spatial distribution of PWV across a PC slab surface with submicron spatial resolution for label-free imaging. The PCEM imaging system is integrated with an ordinary inverted light microscope. The non-coherent light is emitted from a LED, and line-profiled with a cylindrical lens and p-polarized with a polarized beam splitter (PBS), then illuminated from beneath the PC slab biosensor for live-cell imaging. A motorized translation is used to perform the line-scan. A charge-coupled device (CCD) camera combined with an imaging spectrometer is utilized to collect the spectral data for each voxel.

3. Results and Discussions

An attractive application for PCEM is to build a quantitative cellular library with dynamic adhesion phenotypes for a wide range of attachable cells, which will be invaluable for cellular identification, classification, labeling, and other biosensing uses. Figure 1 illustrates a small sample (N=5 cells for each type) of this library as a proof-of-

concept with three different types of stem/progenitor cells (mHAT, 32D, and ASC) and one type of brain cancer cell line (U87-MG). In their undifferentiated state, these cells display morphologies distinct from each other: large, spread-out, rounded shape (mHAT); small, round shape (32D); elongated, spindled shape (ASC); and star-like shape (U87-MG). Figure 1 plots the effective mass density (MD) and brightfield (BF) images measured with PCEM for these four types of cells in the beginning (~8 min) and end (~80 min) of the adhesion process, which clearly demonstrates adhesion features that are very distinct with respect to their cellular types.

As shown in Figure 2 with mean and standard deviation values of adhesion parameters, mHAT cells (in gray) are a murine dental epithelial stem cell line differentiates to form an epithelium, and they tend to adhere tightly onto a PC substrate (e.g., high intensity of effective mass density ~40 fg/μm^3), spread rapidly with large adhesion areas (e.g., spread from ~10 μm^2 to ~3000 μm^2), and exhibit low adhesion eccentricities (e.g., ~0.6, which means that the cell morphology is more round compared to the other three types). 32D cells (in blue) are a murine interleukin-3 (IL-3) dependent myeloid progenitor cell line that is widely used as an in vitro model of hematopoiesis as they spontaneously differentiate to granulocytic neutrophils upon the removal of IL-3 and introduction of granulocyte-colony stimulating factor (G-CSF) in the culture media. As with many types of hematopoietic cells, 32D cells are not anchorage-dependent cells and regarded only very weakly adherent, rendering adhesion phenotyping of these cells very challenging. PCEM, however, could parse out attachment and adhesion patterns for 32D cells with high spatial and temporal resolution. As expected with non anchorage-dependent cells, 32D cells demonstrate only weak adhesion (e.g. low intensity of effective mass density ~5 fg/μm^3) possibly due to high motility (e.g. high centroid displacement ~20 μm in 80 minutes), and nearly non-spreading adhesion area (e.g., ~100 μm^2). Porcine adipose-derived stem cells (ASC) (in red) can differentiate to adipogenic, osteogenic, and chondrogenic lineages, and they form a spindle shape in their undifferentiated state, with middle-scale adhesion areas (e.g. ~1000 μm^2), high eccentricities (e.g. ~0.9, which means the cell is more elongated), and middle-scale mass density (e.g., ~15 fg/μm^3) on a PC surface. Finally, U87-MG cells (in green) are a human primary glioblastoma cell line derived from malignant gliomas and widely used as an in vitro model to study glioblastoma multiforme (GBM), which is the most common and most aggressive form of brain cancer with rapid, diffuse infiltration, and is responsible for low patient survival rates that have remained unchanged for decades. U87-MG cells show star-like morphology with multiple

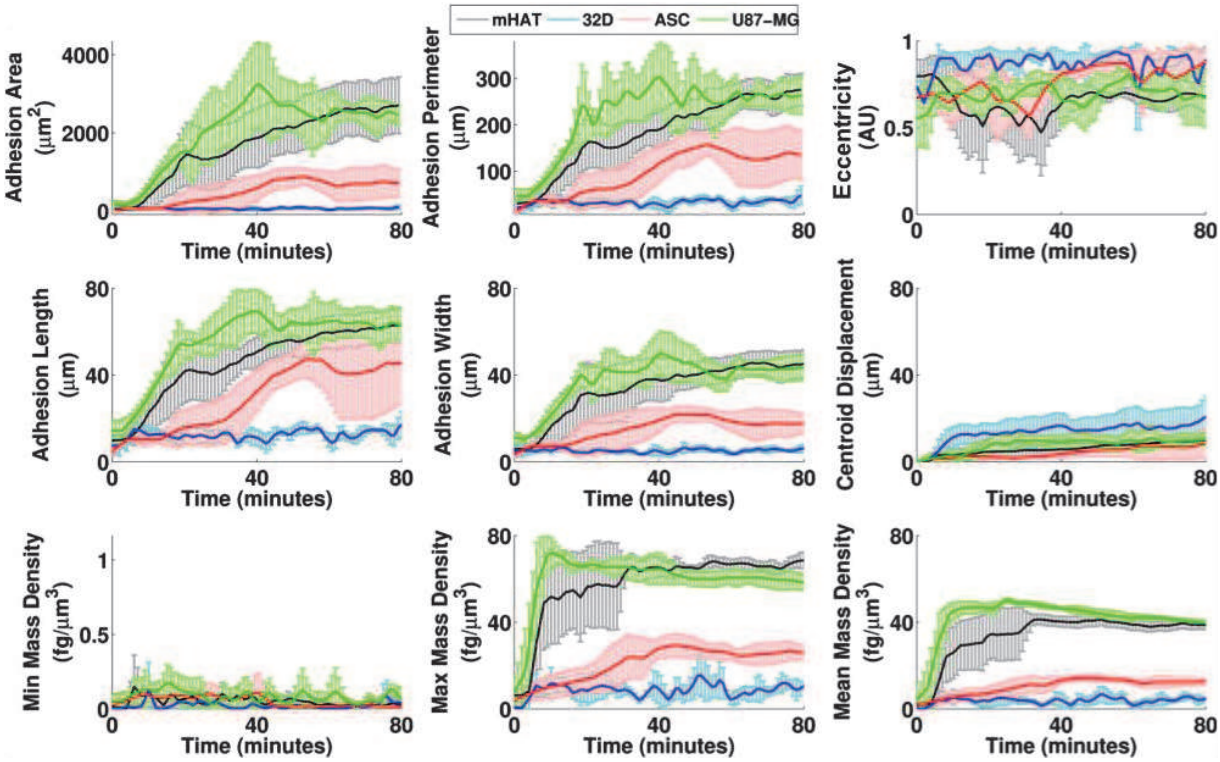

Fig. 2. Plots the mean and standard deviation along time dimension (0~80 min) of membrane-associated effective mass density (MD) images of three different types of stem cells and one type of cancer cells: mHAT, 32D, ASC, U87-MG. Statistical comparison of attached cellular materials for different types of cells, including eccentricities, attached cellular areas/perimeters/length/width/centroid displacement, and min/max/mean effective mass density values (N=5 cells for each type).

spindles (high eccentricities of ~0.8), and rapidly spread to a relatively large adhesion area (e.g., spread from ~10 μm^2 to ~2000 μm^2) while showing tight adhesion (e.g., high intensity of effective mass density ~40 $fg/\mu m^3$). Statistical information (Figure 3) extracted from the curves in Figure 2 at the beginning and end of the adhesion process (T1=~8 min, T2=~80 min) successfully quantifies and characterizes the unique dynamic adhesion phenotypes of these four types of cells. Such quantitative phenotyping information of dynamic cell adhesion can be utilized to study the mechanisms of cell-substrate interactions, as well as offering a novel means to identify cell populations based on their adhesion profiles, possibly opening up new avenues for bioengineering applications in vitro.

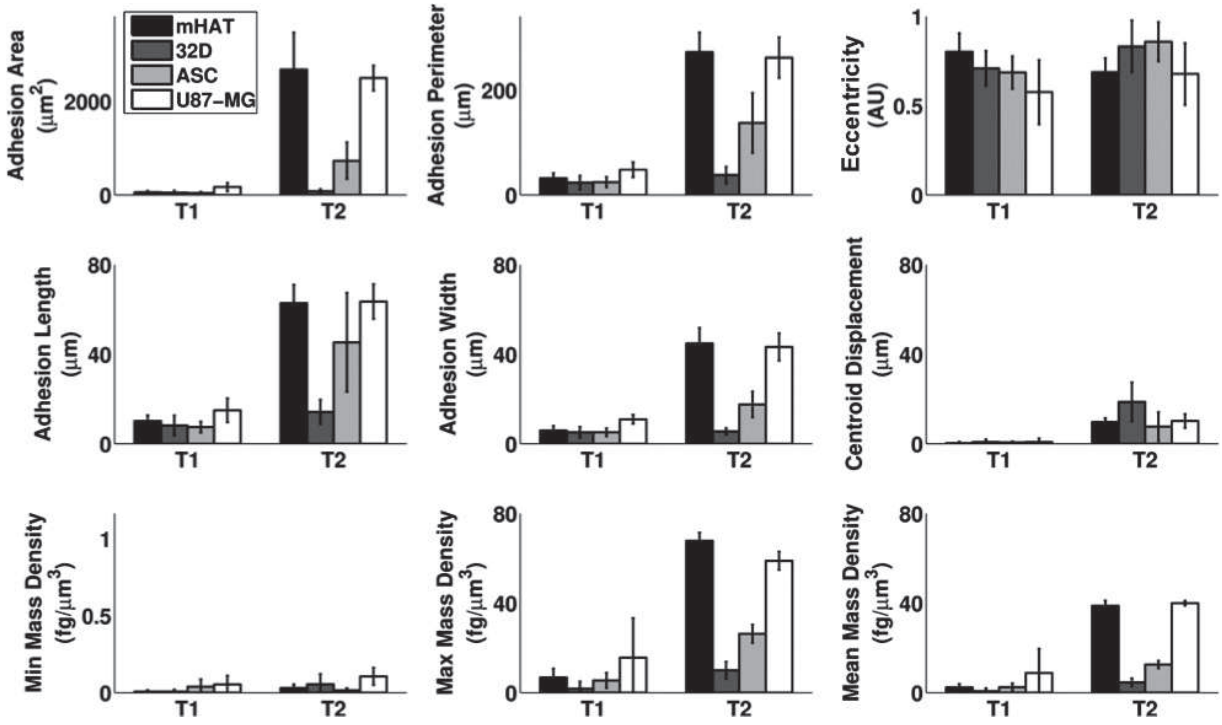

Fig. 3. Plots two different time points (T1=8 min, T2=80 min) of membrane-associated effective mass density (MD) images of three different types of stem cells and one type of cancer cells: mHAT, 32D, ASC, U87-MG. Statistical comparison of attached cellular materials for different types of cells, including eccentricities, attached cellular areas/perimeters/length/width/centroid displacement, and min/max/mean effective mass density values (N=5 cells for each type).

4. Conclusions

To summarize, PCEM can dynamically monitor and quantitatively measure cell-surface interactions and cellular membrane-associated effective mass density transport behavior with high sensitivity, high axial spatial resolution, and sufficiently high lateral spatial resolution to clearly observe attachment feature evolution within individual cells. PCEM is a new tool for measuring single-cell behavior that may hold great potential for studying cell-surface attachment profiles, cell-substrate interactions and cell-drug responses. By gathering similar information for multiple cell types, ECM materials, and environmental conditions, our goal is to use PCEM to enable the construction of a "quantitative live cell footprint library" and provide a useful resource for biomedical and biomaterial research.

References

[1] Cunningham, B., Li, P., Lin, B. & Pepper, J. Colorimetric resonant reflection as a direct biochemical assay technique. Sensor Actuat B-Chem 81, 316-328 (2002).
[2] Cunningham, B. et al. A plastic colorimetric resonant optical biosensor for multiparallel detection of label-free biochemical interactions. Sensor Actuat B-Chem 85, 219-226 (2002).
[3] Chen, W. et al. Photonic crystal enhanced microscopy for imaging of live cell adhesion. The Analyst 138, 5886-5894 (2013).
[4] Zhuo, Y. et al. Single nanoparticle detection using photonic crystal enhanced microscopy. The Analyst 139, 1007-1015 (2014).
[5] Zhuo, Y. & Cunningham, B. T. Label-Free Biosensor Imaging on Photonic Crystal Surfaces. Sensors (Basel) 15, 21613-21635 (2015).